Hindawi Publishing Corporation
International Journal of Electrochemistry
Volume 2014, Article ID 239270, 6 pages
http://dx.doi.org/10.1155/2014/239270

Research Article

Pd-Au Electrocatalysts for Hydrogen Evolution Reaction at Neutral pH

Elitsa Chorbadzhiyska,[1] Mario Mitov,[1] Georgi Hristov,[1] Nina Dimcheva,[2] Lori Nalbandian,[3] Antigoni Evdou,[3] and Yolina Hubenova[4]

[1] *Department of Chemistry, South-West University "Neofit Rilski", 2700 Blagoevgrad, Bulgaria*
[2] *Department of Physical Chemistry, Plovdiv University "Paisii Hilendarski", 4000 Plovdiv, Bulgaria*
[3] *Laboratory of Inorganic Materials (LIM), Chemical Process & Energy Resources Institute, Center for Research and Technology-Hellas (CPERI/CERTH), Thermi, 57001 Thessaloniki, Greece*
[4] *Department of Biochemistry and Microbiology, Plovdiv University "Paisii Hilendarski", 4000 Plovdiv, Bulgaria*

Correspondence should be addressed to Mario Mitov; mitovmario@mail.bg

Received 31 December 2013; Revised 23 February 2014; Accepted 10 March 2014; Published 31 March 2014

Academic Editor: Benjamín R. Scharifker

Pd-Au codeposits with different ratio of both metals were electrodeposited on carbon felt, characterized by scanning electron microscopy, and investigated as electrocatalysts towards hydrogen evolution reaction in neutral phosphate buffer solution. The quantities of the produced hydrogen gas with different electrocatalysts, estimated from data obtained by chronoamperometry, were confirmed by mass spectrometry analysis. The highest hydrogen evolution rate was achieved with the electrocatalysts, produced from electrolyte with equal Pd and Au content.

1. Introduction

Hydrogen evolution reaction (HER) takes place at the cathode in many industrial electrolysis processes with aqueous electrolytes. The choice of cathode material strongly affects the kinetics of HER as the exchange current density on different metals varies several orders of magnitude [1]. This is especially important for some innovative technologies such as microbial electrolysis cells (MECs) [2] and solar water splitting cells [3], where hydrogen production is the main target. Although the cathode process in MEC is the same as that of a water electrolyzer [4], the operational conditions in both systems are completely different [5]. Due to the lower overpotential, most of the cathode materials applied in water electrolyzers and other industrial electrochemical devices have been tested in strongly alkaline or acidic electrolytes. Only a few studies have been performed in neutral solutions, required for bioelectrochemical systems (BES) like MEC. As the MECs use the same bioanodes as those in microbial fuel cells (MFCs), the crucial point for their practical application is to find effective cathodic catalysts at neutral electrolytes [6].

Platinum is well known as the best electrocatalyst for HER and has been widely employed as the cathodic catalyst in MECs [7, 8]. The use of platinum, however, is not to be preferred because of its high cost and easy poisoning by chemicals, such as sulfide, which is a common constituent of wastewater. Numerous other metals and their alloys have been investigated as alternative cathode materials [6]. Kye et al. [9] have demonstrated that Pt-Au electrocatalyst shows higher area-specific activity than platinum nanoparticles alone. Palladium, being the most platinum-like metal with excellent catalytic property and high abundance, is also of key importance. Recently, Huang et al. [10] reported that Pd nanoparticles coated carbon cloth was almost 50 times more effective than Pt as cathode catalyst for HER in MEC.

In this study, Pd-Au composites were electrodeposited on carbon felt and tested as electrocatalysts for HER in neutral phosphate buffer solution (PBS). The results obtained by means of mass spectrometry (MS) analysis and chronoamperometric measurements were compared and the influence of the palladium and gold ratio on the hydrogen evolution rate was discussed.

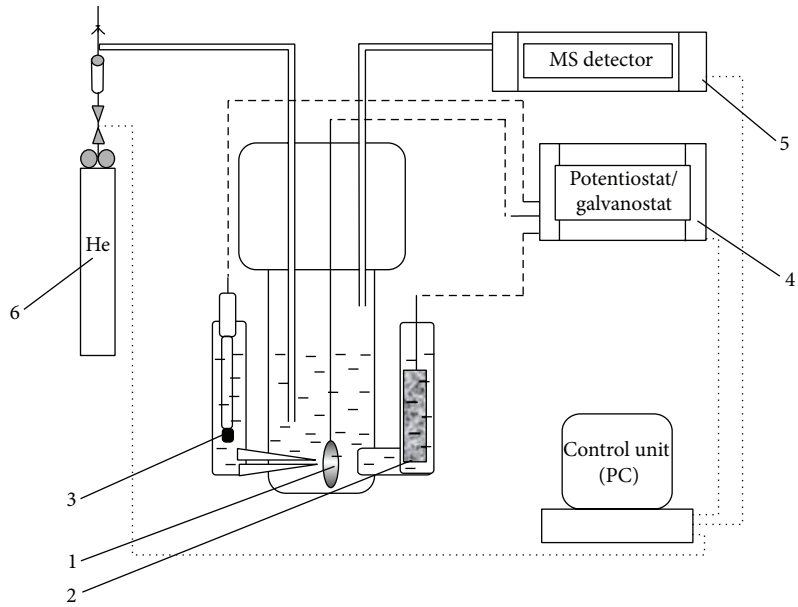

Figure 1: Experimental setup: (1) working electrode, (2) counterelectrode, (3) reference electrode, (4) potentiostat/galvanostat, (5) MS detector, and (6) gas-carrier.

2. Materials and Methods

2.1. Production and Characterization of Pd-Au Electrodeposits. Electrodes were prepared by electrochemical codeposition of Pd and Au on carbon felt (SPC-7011, 30 g/m^2, Weißgerber GmbH & Co. KG) with geometric area of 1 cm^2 from electrolytes consisting of 2% $PdCl_2$ in 0.1 M HCl and 2% $HAuCl_4$ in 0.1 M HCl, mixed in volume ratios 90 : 10, 70 : 30, and 50 : 50 [11], and will be further denoted in the text as $Pd_{90}Au_{10}$; $Pd_{70}Au_{30}$; and $Pd_{50}Au_{50}$, respectively. The electrodeposition was carried out in potentiostatic regime ($E_{deposit}$ = −155 mV versus Ag/AgCl, 10 s) by using PalmSens handheld potentiostat/galvanostat.

The morphology of the developed materials was analyzed by scanning electron microscopy (SEM) using JEOL 6300.

The extent of electrochemical accessibility determines the practical utilization of the high surface area electrode materials [12]. The electrochemical accessible surface area (ECSA) of the produced materials was determined by means of cyclic voltammetry (CV), performed in the potential region, where only nonfaradaic currents were observed. The capacitance charging current densities were measured at the middle of the scan range and the double layer capacitance calculated from the slope of the linear part of the charging current density against the scan rate [13]. The ECSA was estimated using the following equation:

$$\text{ECSA} = \frac{C}{C_{sp}}, \quad (1)$$

where C is the determined capacitance and C_{sp} is the specific capacitance, which for the carbonaceous material is taken to be 25 μF/cm^2 [12].

2.2. Experimental Setup and Procedures. The electrocatalytic activity of the prepared materials towards HER was investigated by means of linear voltammetry (LV) with scan rate 2 mV/s over the potential range from 0 to −1.2 V (versus Ag/AgCl) in 67 mM PBS (pH 7.0). The electrochemical experiments were carried out in a three-electrode cell (Figure 1). The electrode samples were connected as a working electrode (1) and a platinum-titanium mesh (10 cm^2) was used as a counterelectrode (2). All potentials were measured against Ag/AgCl (3 M KCl) reference electrode (3). The electrochemical studies were performed by using PalmSens handheld potentiostat/galvanostat (4). LV scan was repeated three times for each sample and the third scan was used for data analysis. The evaluation of the performance was based on the voltage needed to initiate hydrogen production (V_e) and the slope (V_h) of the first linear region in the voltammogram.

In parallel, chronoamperometric measurements were carried out under the same conditions. The working electrode was polarized from −500 mV to −1200 mV (versus Ag/AgCl) with a voltage step of 100 mV for 10 min at each step and the current was monitored. The electrochemical cell gas outlet was connected to quadruple mass spectrometer (Baltzers-Omnistar) for continuous quantitative analysis of the produced gases (5). Helium, at flow rate 40 cm/min, was used as a gas-carrier (6). The mass-spectrometer response was calibrated by 6 injections of pure substance (H_2) using a 4-way valve equipped with a 100 μL loop. The mass fractions corresponding to water (m/e: 18, 17, 16), hydrogen (m/e: 2), nitrogen (m/e: 28, 14), oxygen (m/e: 32, 16), carbon monoxide (m/e: 28, 12), carbon dioxide (m/e: 44, 28, 12), and nitrogen oxides (m/e: 30) were monitored during each experiment. The reaction products were measured during each potential pulse and integrated for the whole pulse duration.

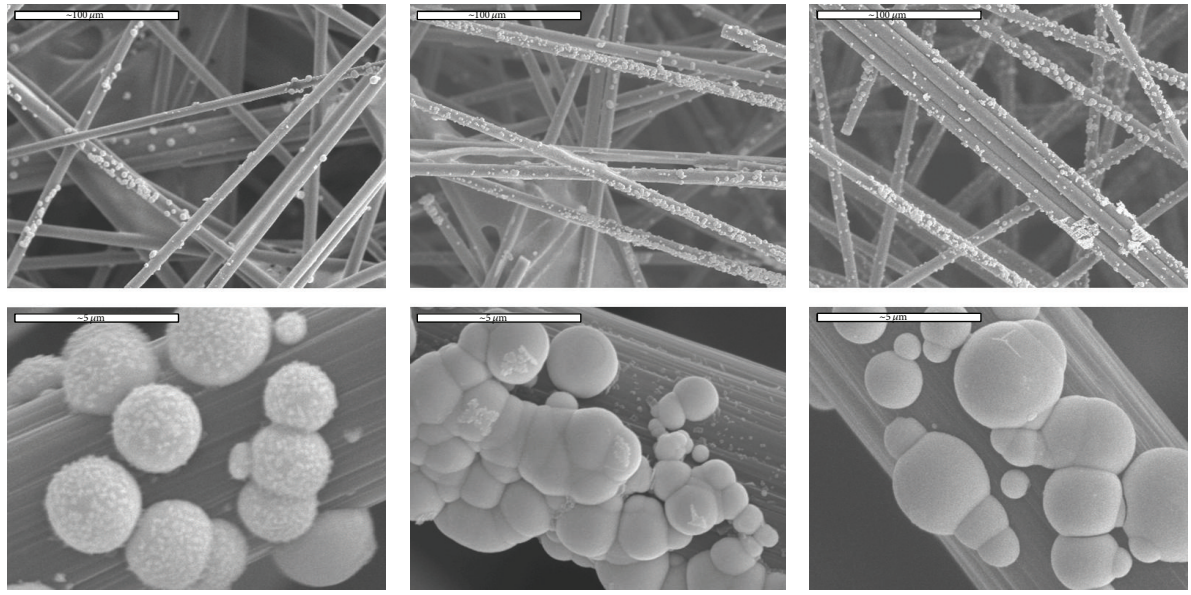

Figure 2: SEM images of the Pd-Au electrodeposits on carbon felt: (a) $Pd_{90}Au_{10}$; (b) $Pd_{70}Au_{30}$; (c) $Pd_{50}Au_{50}$.

The quantity of the produced hydrogen was estimated from the areas corresponding to the $m/e = 2$ MS response.

3. Results and Discussion

The catalysts activity depends not only on the elemental content, but also on the method of preparation, morphology, catalyst support, and so forth. Scanning electron microscopy showed that the supporting material (carbon felt) itself has a fiber-like structure, which provides significant active surface. The Pd-Au electrodeposits are irregularly distributed over the carbon fibers forming islands with varying size (Figures 2(a), 2(b), and 2(c)—top). A bigger magnification of the codeposits revealed that the islands consist of near spherical complex structures sizing up to 2.5 micrometers (Figures 2(a), 2(b), and 2(c)—bottom). Earlier studies [14] have proved that each globular structure is formed by large number of nanosized particles, whose shape is strongly affected by the percentage of gold in the deposit and changes from needle-like crystallites (as with the codeposits with high Pd content) to cauliflower-like shape, observed with Au-enriched crystallites. In the same paper [14], the XRD spectra of Pd-Au codeposits produced in varied proportion of the both metals were compared with those of the pure Au and Pd electrodeposits. The 2Θ values of the deposits indicate the availability of *fcc* crystalline metal phases corresponding to (111), (200), and (220) facets. The diffraction peaks of the codeposited metal phases were shifted to the lower 2Θ values as compared to that of the pure Pd. The lattice expansion caused by the inclusion of Au atoms into the Pd *fcc* structure is indicative for the alloys formation.

In order to compare the electrocatalytic activity of the produced electrodeposits, the ECSA values were estimated (Figure 3(a)) based on the CVs performed with the investigated materials in the potential range (0.2 ÷ 0.7 V versus Ag/AgCl), where nonfaradaic reactions take place (Figure 3(b)). The increase of the ECSA with that of Pd content coincides with the upper described changes of the electrodeposits' morphology. All further results, concerning electrocatalytic properties towards HER, are normalized against ECSA of each electrode.

Table 1: Current density (mA cm^{-2}) for hydrogen evolution reaction (HER) for investigated electrodes in 67 mM PBS (pH 7.0).

Sample	Current density (−1.2 V)/mA cm^{-2}
Carbon felt	0.049 ± 0.007
$Pd_{90}Au_{10}$/carbon felt	0.145 ± 0.012
$Pd_{70}Au_{30}$/carbon felt	0.255 ± 0.010
$Pd_{50}Au_{50}$/carbon felt	0.415 ± 0.015

Linear voltammograms (LVs) obtained with the newly produced Pd-Au modified and nonmodified carbon felt electrodes are compared in Figure 4. The LVs indicated that by sweeping the potential more negative than −0.5 V (versus Ag/AgCl) the cathodic current for all modified carbon felt electrodes gradually increased. The values of current density deduced from Figure 4 at −1.20 V (versus Ag/AgCl) are given in Table 1, taking into account the electrochemical accessible surface area of each electrode.

The obtained results for the values of V_e and V_h, estimated from LVs, are presented in Figure 5. The value of V_e indicates the relative overpotential, while V_h reflects current production rate at an applied voltage. Best catalyst performance is achieved at a low V_e and large V_h value [15]. All Pd-Au modified electrodes, investigated in this study, exhibited better performance than the bare carbon felt in neutral

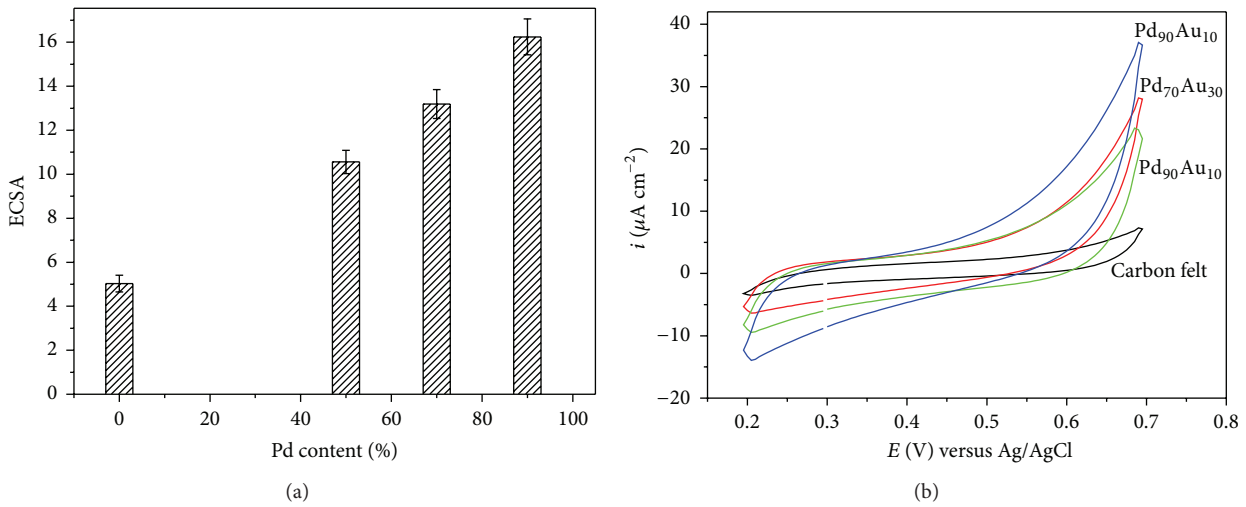

FIGURE 3: (a) Variation of ECSA with Pd content; (b) cyclic voltammograms obtained with Pd-Au in different ratios on carbon felt in phosphate buffer (pH 7.0); scan rate 10 mV/s (current density is calculated with respect to the electrode geometric area).

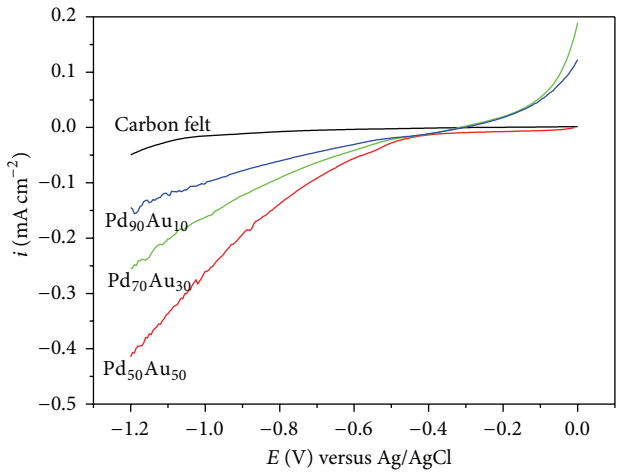

FIGURE 4: Linear voltammograms obtained with Pd-Au electrodeposits on carbon felt in neutral phosphate buffer (the current density is normalized against ECSA).

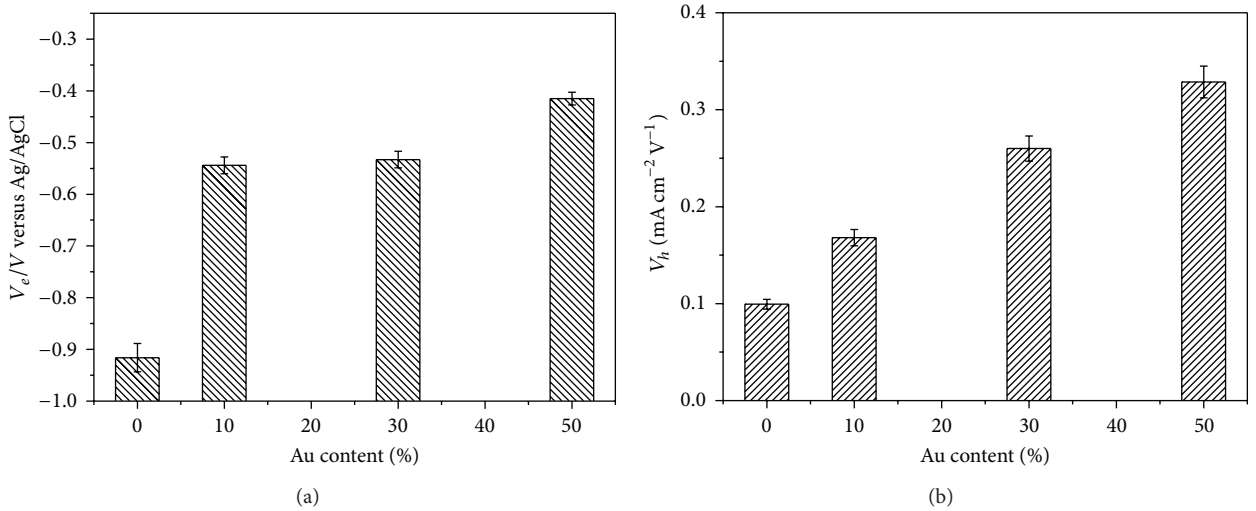

FIGURE 5: Variation of the estimated (a) V_e; (b) V_h values with the Au content.

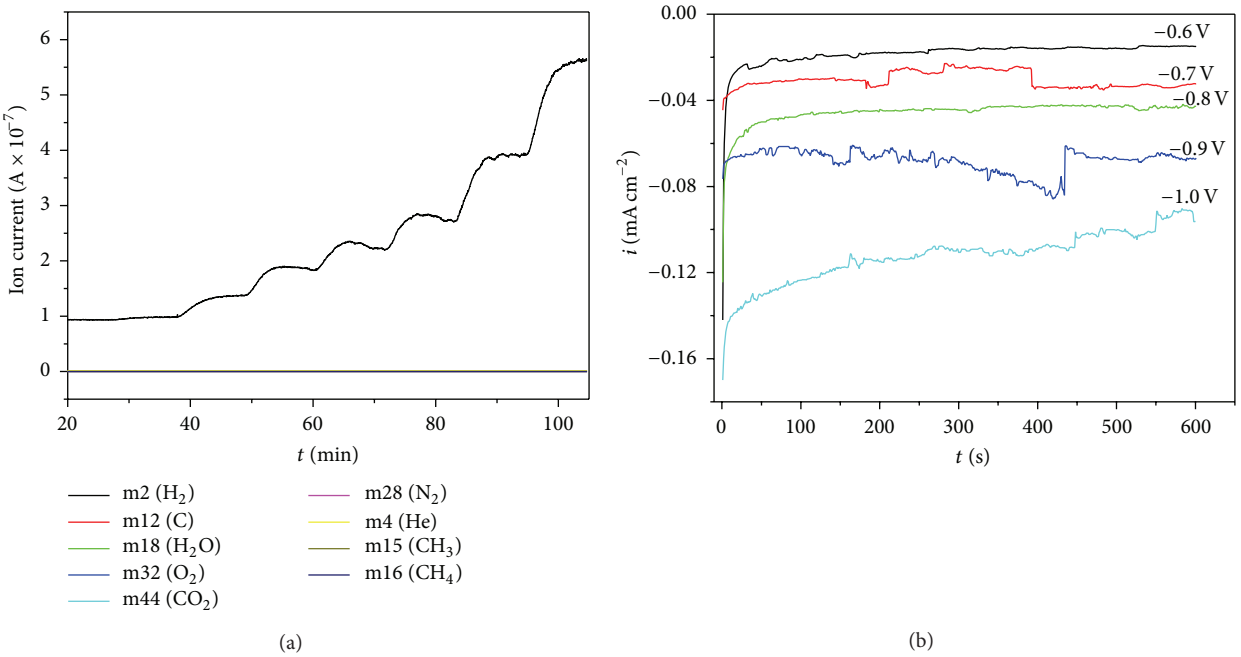

(a) (b)

FIGURE 6: (a) MS diagram; (b) chronoamperograms obtained at different applied potentials with Pd-Au/carbon felt electrode.

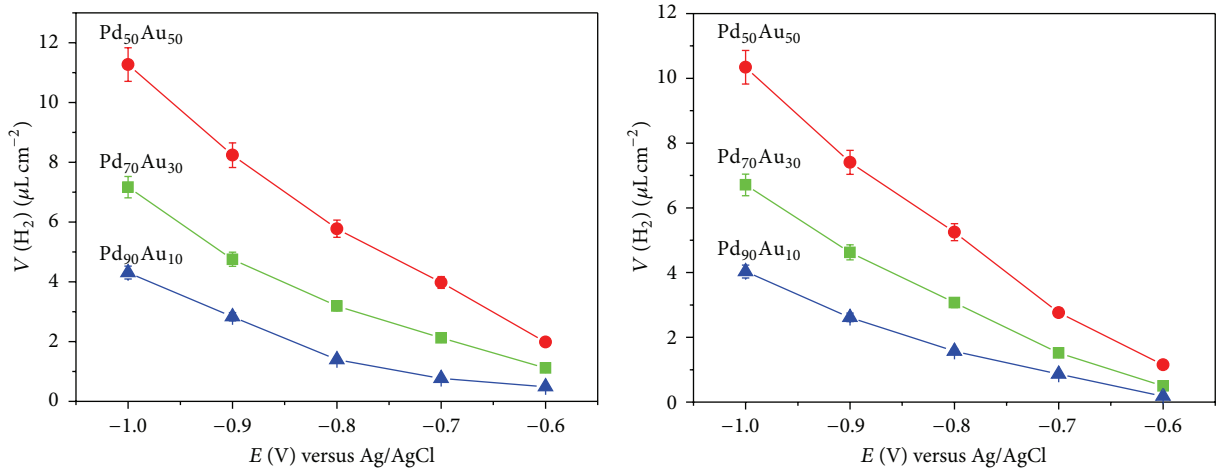

(a) (b)

FIGURE 7: Quantities of evolved hydrogen at different applied potentials estimated from (a) MS data; (b) chronoamperometric measurements.

phosphate buffer. The minimum voltage needed to initiate substantial current (V_e) was in the range between −0.42 V and −0.54 V versus Ag/AgCl for all modified electrodes (Figure 5(a)), which is lower than that reported for Pt/carbon cloth in phosphate buffer [15]. Comparing the hydrogen production rate values (Figure 5(b)), the examined materials can be ranked as follows: $Pd_{90}Au_{10}$ < $Pd_{70}Au_{30}$ < $Pd_{50}Au_{50}$.

This order was proved by the experiments, in which the current response was monitored at different potentials and in parallel the produced gases were analyzed by a MS detector. A MS diagram obtained in such experiment with Pd-Au/carbon felt electrode is shown in Figure 6(a). Only the signal reflected to hydrogen was changed during the experiment, which enhanced when the electrode potential was shifted to more negative values. No changes in the signals referring to other analyzed gas components were detected, which excluded their participation in the cathodic reaction.

The quantity of the produced hydrogen was independently calculated in two ways: first, based on the area of the corresponding mass spectrometer signals, m/e = 2 (Figure 5(a)), and second, by integration of areas under chronoamperometric curves obtained at each potential (Figure 6(b)) and applying Faraday's law. The results obtained by both independent methods are comparable for all studied electrode materials (Figures 7(a) and 7(b)), which verifies

the reliability of the chronoamperometric measurements. A tendency for increasing the amount of generated hydrogen with the decrease of palladium and enrichment of gold in the electrodeposited catalysts is observed. This effect of the partial substitution of Pd with Au with respect to the electrocatalytic activity towards HER could be assigned to diminishing the well-known high capability of the palladium for hydrogen absorption and hydride formation, which is established not only for the bulk metal, but also for Pd nanoparticles [16].

4. Conclusions

Palladium-gold alloys can be easily produced by electrodeposition on carbon felt. The increase of the gold content in the electrolyte bath enhances the electrocatalytic activity of the obtained electrodeposits towards HER in neutral phosphate buffer solution. The highest catalytic activity was achieved with $Pd_{50}Au_{50}$ electrodeposits. Based on the results obtained in this study we considered that Pd-Au codeposits are promising electrocatalysts for hydrogen generation from neutral electrolytes, which is a prerequisite for their further investigation as cathodes in MECs.

Conflict of Interests

The authors declare that there is no conflict of interests regarding the publication of this paper.

Acknowledgments

This study was supported by the European Territorial Cooperation Program "Greece-Bulgaria 2007–2013" through a Contract B1.33.01 (Project "Hydrogen Economy Cooperation Network for Research-Public Awareness-Business Opportunities across Greek-Bulgarian borders-HYDECON"). The authors also acknowledged the support from the Bulgarian National Science Fund (Grant DVU-02/38).

References

[1] V. S. Bagotsky, *Fundamentals of Electrochemistry*, John Wiley & Sons, Hoboken, NJ, USA, 2nd edition, 2006.

[2] H. Liu, H. Hu, J. Chignell, and Y. Fan, "Microbial electrolysis: novel technology for hydrogen production from biomass," *Biofuels*, vol. 1, no. 1, pp. 129–142, 2010.

[3] M. G. Walter, E. L. Warren, J. R. McKone et al., "Solar water splitting cells," *Chemical Reviews*, vol. 110, no. 11, pp. 6446–6473, 2010.

[4] H. Hu, Y. Fan, and H. Liu, "Hydrogen production using single-chamber membrane-free microbial electrolysis cells," *Water Research*, vol. 42, no. 15, pp. 4172–4178, 2008.

[5] H. Liu, H. Hu, J. Chignell, and Y. Fan, "Hydrogen production in single chamber tubular microbial electrolysis cells using non-precious metal catalysts (NiMo, NiW)," *International Journal of Hydrogen Energy*, vol. 34, no. 20, pp. 8535–8542, 2009.

[6] A. Kundu, J. N. Sahu, G. Redzwan, and M. A. Hashim, "An overview of cathode material and catalysts suitable for generating hydrogen in microbial electrolysis cell," *International Journal of Hydrogen Energy*, vol. 38, no. 4, pp. 1745–1757, 2013.

[7] S. Cheng and B. E. Logan, "Sustainable and efficient biohydrogen production via electrohydrogenesis," *Proceedings of the National Academy of Sciences of the United States of America*, vol. 104, no. 47, pp. 18871–18873, 2007.

[8] H. Liu, S. Grot, and B. E. Logan, "Electrochemically assisted microbial production of hydrogen from acetate," *Environmental Science and Technology*, vol. 39, no. 11, pp. 4317–4320, 2005.

[9] J. Kye, M. Shin, B. Lim, J. W. Jang, I. Oh, and S. Hwang, "Platinum monolayer electrocatalyst on gold nanostructures on silicon for photoelectrochemical hydrogen evolution," *ACS Nano*, vol. 7, no. 7, pp. 6017–6023, 2013.

[10] Y.-X. Huang, X.-W. Liu, X.-F. Sun et al., "A new cathodic electrode deposit with palladium nanoparticles for cost-effective hydrogen production in a microbial electrolysis cell," *International Journal of Hydrogen Energy*, vol. 36, no. 4, pp. 2773–2776, 2011.

[11] E. Horozova, T. Dodevska, N. Dimcheva, and R. Mussarlieva, "Electrocatalytic reduction of hydrogen peroxide on palladium-gold codeposits on glassy carbon: applications to the design of interference-free glucose biosensor," *International Journal of Electrochemistry*, vol. 2011, Article ID 697698, 8 pages, 2011.

[12] S. Brocato, C. Lau, and P. Atanassov, "Mechanistic study of direct electron transfer in bilirubin oxidase," *Electrochimica Acta*, vol. 61, pp. 44–49, 2012.

[13] S. M. Fernández-Valverde, E. Ordoñez-Regil, G. Cabañas-Moreno, and O. Solorza-Feria, "Electrochemical behavior of Ni-Mo electrocatalyst for water electrolysis," *Journal of the Mexican Chemical Society*, vol. 54, no. 3, pp. 169–174, 2010.

[14] T. C. Nagaiah, D. Schäfer, W. Schuhmann, and N. Dimcheva, "Electrochemically deposited Pd-Pt and Pd-Au Codeposits on graphite electrodes for electrocatalytic H_2O_2 reduction," *Analytical Chemistry*, vol. 85, no. 16, pp. 7897–7903, 2013.

[15] Y. Zhang, M. D. Merrill, and B. E. Logan, "The use and optimization of stainless steel mesh cathodes in microbial electrolysis cells," *International Journal of Hydrogen Energy*, vol. 35, no. 21, pp. 12020–12028, 2010.

[16] E. A. Crespo, M. Ruda, S. Ramos de Debiaggi, E. M. Bringa, F. U. Braschi, and G. Bertolino, "Hydrogen absorption in Pd nanoparticles of different shapes," *International Journal of Hydrogen Energy*, vol. 37, no. 19, pp. 14831–14837, 2012.